Return to Session

MEASUREMENT AND MODELING OF SPACE CHARGE ACCUMULATION IN POLYMERIC HVDC CABLE SYSTEMS

Riccardo BODEGA, Prysmian Cables and Systems, The Netherlands, riccardo.bodega@prysmian.com
Peter MORSHUIS, Delft University of Technology, The Netherlands, p.h.f.morshuis@tudelft.nl
Gabriele PEREGO, Prysmian Cables and Systems, Italy, Gabriele.perego@prysmian.com

ABSTRACT

This paper describes a numerical model for the calculation of the dynamic electric field distribution in high-voltage (HV) direct current (DC) cable insulation. The model includes space charge phenomena in the insulation bulk and at dielectric interfaces, such as those encountered in cable accessories. The numerical modelling has been supported by laboratory measurements of space charge and electric field. Theoretical and experimental results pointed out that both the temperature and the temperature gradient experienced by the insulation have a significant effect on the time-dependent distribution of the electric stress in the cable system.

KEYWORDS

HVDC, DC, cable, cable system, interface, space charge, temperature gradient.

INTRODUCTION

Accumulation of space charge plays a major role in determining the electric field distribution in the insulation of polymeric HVDC cable systems. In fact, if space charge is present, the total electric field across the insulation is given by both the Laplacian and the space-charge field. If space charge accumulation is not controlled, the total electric field can be locally enhanced, affecting significantly the performance of the insulation system.

In this paper a model is presented for the calculation of space charge dynamics in cables and at dielectric interfaces, such as those encountered in joints and terminations. The model predicts space charge accumulation on the basis of macroscopic properties of the cable insulation, e.g. permittivity and conductivity. By considering those quantities as functions of temperature and electric field, the model is able to calculate the space charge accumulation for different cable loads and for different voltage conditions, including the voltage polarity reversal.
The model has been validated by means of space charge measurements performed on cable models (medium-voltage size) and on models of dielectric interfaces. To that purpose, the pulsed electro-acoustic (PEA) method [1] has been used for the measurements. Space charge profiles and the relative electric field plots have been measured for several applied fields and at several temperature conditions, including the case in which the cable insulation experiences a temperature gradient.

NUMERICAL MODEL FOR THE CALCULATION OF SPACE CHARGE AND ELECTRIC FIELD

Background

One of the intrinsic properties of DC cable insulation is the accumulation of charges. Insulating materials allow a weak electrical conduction. This weak flow of charge within the insulation may not be uniform, because of a local non-homogeneity of the material.
According to the current density continuity equation, when an inequality occurs between the flow of charges into a region and the flow of charges out of that region, charge accumulates in that region, see equation (1):

$$\nabla \cdot \vec{j} + \frac{\partial \rho}{\partial t} = 0 \qquad (1)$$

In equation (1), j is the current density, ρ is the charge per unit volume (also called space charge density or simply space charge) and t the time. According to Gauss' law, a space charge field E_ρ is associated to a charge distribution:

$$\rho = \nabla \cdot \left(\varepsilon_0 \ \varepsilon_r \ \vec{E}_\rho \right) \qquad (2)$$

where ε_0 is the vacuum permittivity and ε_r the relative permittivity of the insulation. Therefore, the electric field E within the insulation in the presence of space charge is given by the sum of two contributions: the space charge field and the external field E_0 (also called Laplacian field), which is induced by the applied voltage, see equation (3).

$$\vec{E} = \vec{E}_0 + \vec{E}_\rho \qquad (3)$$

In the AC situation, the flow of charges inverts its direction too quickly to allow a significant growth of space charge at the insulation inhomogeneities, at least for conventional insulating materials. This means that the space charge field can be neglected. On the other hand, under DC stressing condition, the flow of charge maintains the same direction. This allows a build-up of charge, which, in general, significantly affects the electric field distribution inside the insulation.

Polymeric insulation can be considered a weakly conductive continuum in which a non-homogeneity can be induced by a non-uniform applied stress. This is the case of loaded DC cables and of the majority of HVDC devices. In fact, in those components a conductivity gradient is induced by the non-uniform electric field and/or by the temperature drop across the insulation.

The permittivity of the insulation can be assumed constant within the range of temperatures and fields adopted in DC cables [2]. On the other hand, the conductivity σ is to be considered a function of both temperature T and field E: $\sigma=\sigma(T,E)$. The system studied in this work consists of the cable insulation in non-ohmic contact with the electrodes [2]. This is modelled by considering an equivalent insulation in ohmic contact with the electrodes. The conductivity of the equivalent insulation is derived by fitting the conductivity function with the experimental results of conduction current measurements [3]. The measurements have been performed on the system to be modelled, i.e. the cable insulation in non-ohmic contact with the electrodes. In this way, the equivalent insulation includes the effect that the electrodes have on the conduction process. In Figure 1, this concept is schematised.

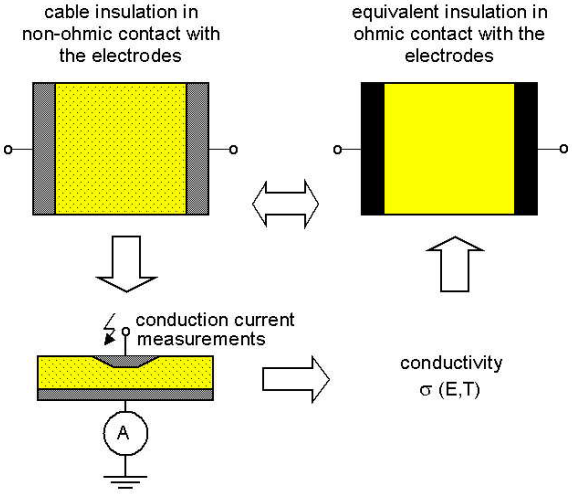

Figure 1: physical model of the insulation.

Model implementation

The model is implemented by means of a numerical procedure. For the procedure it is assumed that the radial space charge distribution within the cable/cable joint is the same along the whole cable, independently on the axial position and on the angular position. Therefore, a one dimensional configuration, which is represented in Figure 2, has been used.

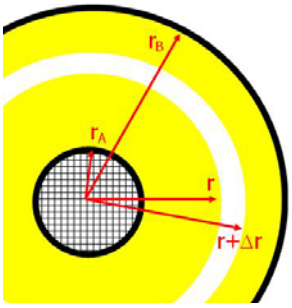

r = generic radius
r_a = inner radius
r_b = outer radius
Δr= thickness of the annulus-shaped partition

Figure 2: model of the insulation used for the numerical procedure.

The insulation is divided into 201 annulus-shaped partitions of thickness Δr (see Figure 2). Each partition is characterized by the following quantities, which are in general function of time t and radius r: temperature $T(t,r)$, electric field $E(t,r)$, current density $J(t,r)$, space charge $\rho(t,r)$, conductivity $\sigma(T(t,r),E(t,r))$.
In case of dielectric interfaces, the interfacial charge $\kappa(t)$, which accumulates at the interfacial radius r_c, is to be considered as well. The above specified quantities are assumed to be constant within each partition and within a time interval Δt. After calculating all quantities for the initial conditions, the time is increased by a time step Δt and the quantities are recalculated. This is repeated until the time has reached a predefined value or the calculation has converged toward a solution. An exponentially increasing time step has been used in order to reduce the number of iterations. The calculation can be assumed converged if the divergence of the current density is smaller than a predefined error. In fact, when the divergence of the current density is zero, the actual electric field is a purely resistively-distributed field. In Figure 3 the flow-chart of the procedure is represented.

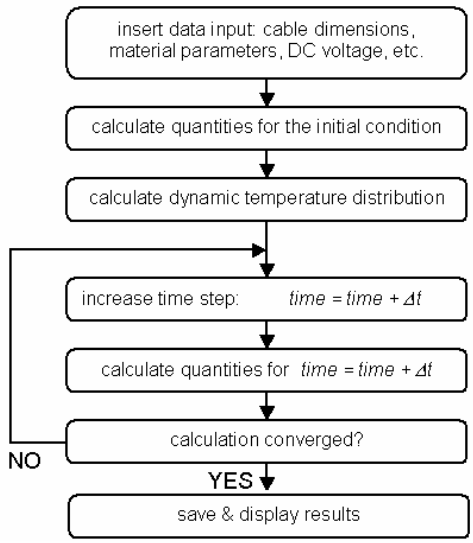

Figure 3: flow-chart of the numerical procedure.

TEST SET-UP ADOPTED FOR THE MEASUREMENTS OF SPACE CHARGE

Test specimens

Space charge measurements were performed on two different types of test specimens: MV-size cables and MV-size models of a dielectric interface.
MV-size cables consisted of 7-m long samples of XLPE cables, with an insulation thickness of 4.5 mm. The cross-section of a MV-size cable is represented in Figure 4.
A picture of a MV-size model of a dielectric interface is represented in Figure 5. Such a specimen is constructed in the following way. Firstly, the earth screen and the outer semicon of an XLPE-insulated cable (area of the inner conductor = 50 mm^2; insulation thickness = 4.5 mm) is scraped off for a length of 80 mm. Then, part of the exposed insulation is removed by means of a glass blade and the insulation surface is smoothed by using successive grades of abrasive cloth. After these operations, the thickness of the remaining XLPE in the central part of the opening is 2 mm. At this point, a 100-mm long elastic tube made of EPR (thickness = 2 mm) can be applied on the XLPE by means of a special tool. After fitting the EPR tube onto a hollow

mandrel placed over the exposed XLPE, the tool pulls back the mandrel. In this way, the EPR tube stretches over the XLPE. To make easy this operation, silicon oil has to be applied at the inner surface of the EPR tube. Finally, an outer semicon is taped on the EPR.

In order to expel volatile cross-linking by-products, all test specimens were thermally treated at 80 °C for 20 days before any testing.

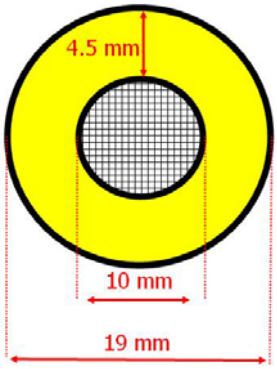

Cable type: triple-extruded

Insulation: XLPE

Conductor: 50 mm2 Al

Length: 12 m

Thermal treatment: 20 days @ 80 °C

Figure 4: Test specimen 1 - MV-size XLPE cable.

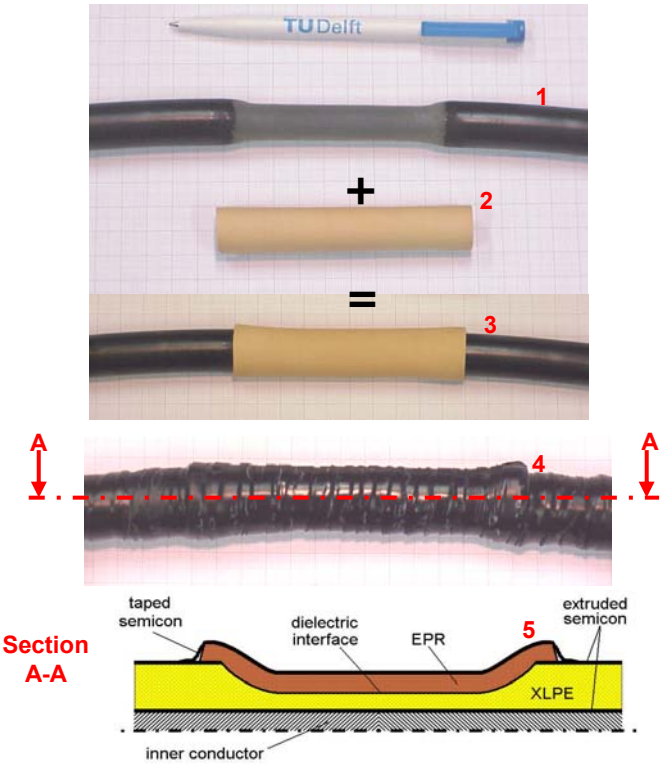

Figure 5: Test specimen 2 - MV-size model of dielectric interface. 1- XLPE cable with exposed insulation; 2- EPR cylinder; 3- cylinder placed onto the cable; 4- semicon tape is applied; 5- cross section of the dielectric interface.

Test method and test conditions

Tests were performed at different temperature conditions and at different values of the applied DC voltage. The induced current-heating technique was used for increasing the temperature of the cable insulation. In this way a temperature gradient between the inner conductor and the outer screen was obtained. The temperature was measured on a dummy loop with the same characteristics as the cable object of the measurement. Four temperature sensors were placed on the dummy loop, two at the conductor and two at the outer semicon. Measurements started only after all sensors had indicated that the temperature had reached a stable value. The Pulsed ElectroAcoustic (PEA) method [1] was used to measure the dynamic space charge distributions. In Figure 6, a picture of the PEA cell adopted in this work is shown, whereas a schematic diagram of the test set up is represented in Figure 7. More details about the test set-up can be found in [4].The test conditions are summarized in Tables 1a and 1b.

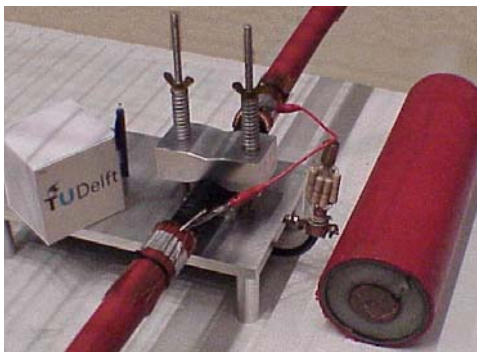

Figure 6: PEA cell adopted in the present work.

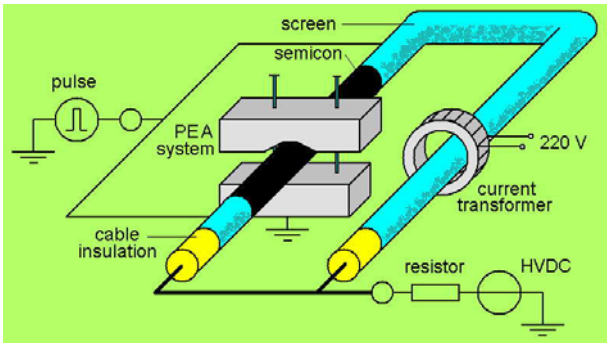

Figure 7: schematic representation of the test set-up used in the present work (drawing not on scale).

Table 1: Test conditions
a) MV-size XLPE cable specimens.

CURRENT LOAD [A]	0	150	220
T_b [°C]	20	30	45
T_a [°C]	20	40	65
ΔT [°C]	0	10	20
∇T [°C /mm]	0	2.2	4.4
VOLTAGE [kV]	22.5	45	90
Voltage polarity	+/-	+/-	+/- and polarity reversal
Electric field (average) [kV/mm]	5	10	20
Polarization time [s]	$2\ 10^4$		

T_b=temperature outer semicon;
T_a=temperature inner semicon;
ΔT =temperature drop;
∇T=average temperature gradient

b) MV-size models of dielectric interfaces.

CURRENT LOAD [A]	0	145	200
T_b [°C]	20	30.1	45
T_a [°C]	20	39.7	65
ΔT [°C]	0	10	20
∇T [°C/mm]	0	2.5	5
VOLTAGE [kV]	40		80
Voltage polarity	+/-		+/- and polarity reversal
Electric field (average) [kV/mm]	10		20
Polarization time [s]	$2\ 10^4$		

RESULTS AND DISCUSSION

1) Temperature distribution

In operation, DC cable systems experience a temperature gradient across their insulation. In Figure 8, a typical temperature profile is shown.

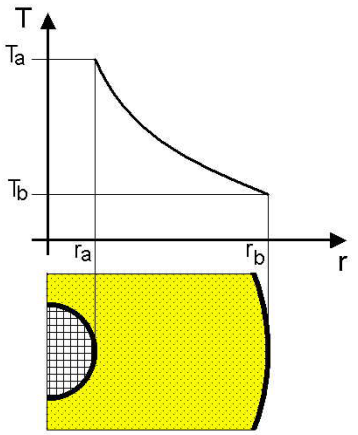

Figure 8: Typical temperature distribution across the insulation of a loaded cable.

Because of the temperature dependency of the insulation conductivity, the conductivity distribution is a decreasing function of the radius if the cable is loaded. Because of this fact, charge with the same polarity as that of the applied voltage is expected to accumulate (e.g. [5,6]). This charge is responsible for the so-called field inversion phenomenon occurring in DC cables, i.e. the electric field is higher near the outer shield rather than near the inner conductor [7].

Experimental results show that both the amount of space charge and its accumulation time depend on the temperature distribution. These facts are direct consequence of the temperature dependency of the insulation conductivity. In the studied situations, the insulation of the cable is not in a macroscopically homogeneous condition. This is mainly because of the fact that the temperature distribution induces a non-homogeneous conductivity. The higher the temperature drop across the insulation, the larger the non-homogeneity of the conductivity and therefore the higher the value of the accumulated space charge. This is shown for MV-size cable specimens in Figure 9, where results of measurements performed at different temperature gradients are presented.

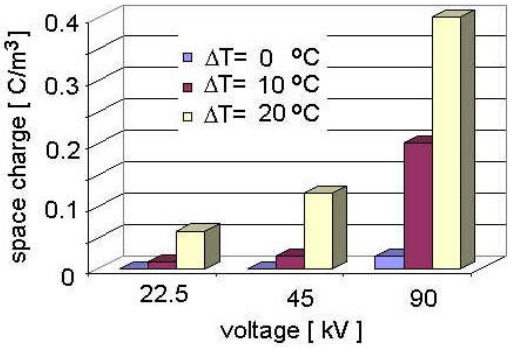

Figure 9. Maximum value of the accumulated space charge in MV XLPE cable specimens after a polarization time of $2\ 10^4$ s.

On the other hand, space charge takes a certain time to accumulate within the insulation. The more conductive the insulation, the faster the space charge accumulation. Since the insulation conductivity strongly increases with the temperature, the higher the absolute value of the temperature, the faster the space charge accumulation. In Figure 10, the evolution in time of space charge, which is measured at specific locations of a loaded cable, is represented and compared with the results of the numerical modeling. The figure shows that the faster space charge accumulation is present in the cable insulation near the inner semicon, where a higher temperature is present.

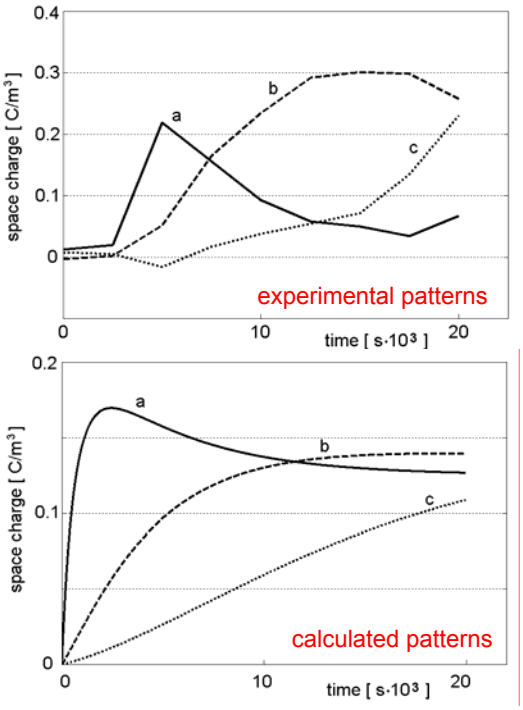

Figure 10: evolution in time of space charge at specific locations in a MV XLPE cable.
a) near the inner semicon; r = 5 mm;
b) in the middle of the insulation; r = 6.75 mm;
c) near the outer semicon; r = 8.5 mm

In Figure 11 experimental results and results of the numerical modeling are compared for MV-size cable specimens. In Figure 12 the same is done, but for MV-size models of interfaces.
Figure 11 shows that an accumulation of positive space charge is well predicted by the model in the insulation bulk due to the presence of the temperature drop. The maximum of the calculated space charge distribution is slightly underestimated and no hetero-charge near the inner semicon is simulated (compare calculated and experimental space charge patterns in Figure 11). However, the calculated and the measured electric field patterns are quite similar: the field inversion phenomenon is in fact predicted by the model.
Regarding Figure 12, the amount of interfacial charge is slightly underestimated by the model. In addition, there is some difference between the charge profiles in the XLPE bulk. Near the inner semicon the model predicts positive charge, whereas no charge has been measured at that location. Despite those facts, the electric field distribution is rather well predicted by the model. In fact, the calculation indicates that the field increases in the EPR and decreases in the XLPE.

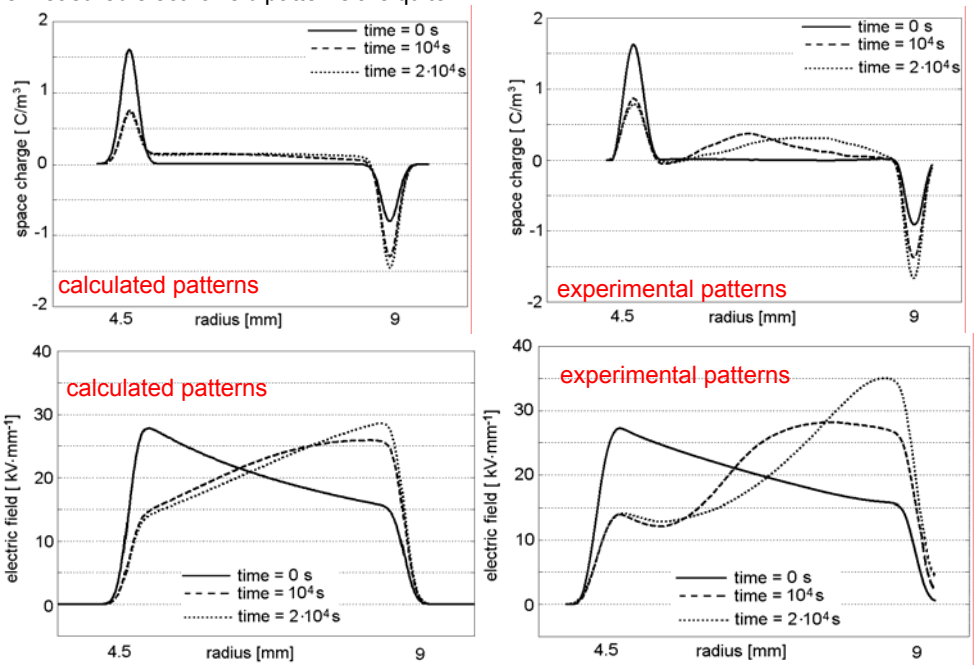

Figure 11: voltage-on space charge patterns and relative electric field profiles for MV-size cable specimens. Calculated patterns and experimental data. V=+90 kV; T_a=65°C, T_b=45°C.

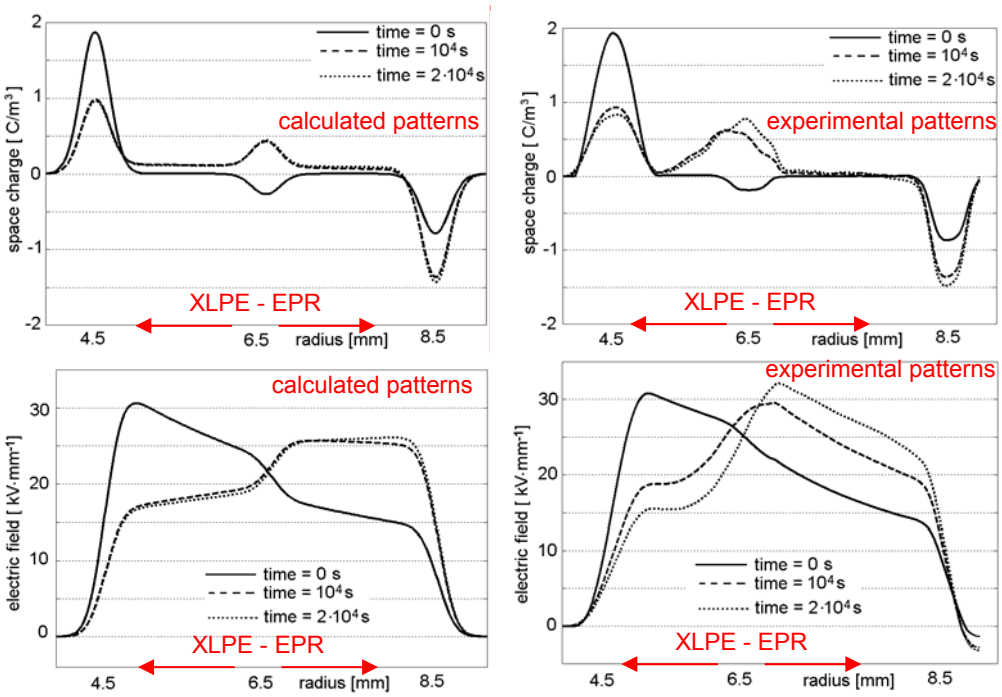

Figure 12: voltage-on space charge patterns and relative electric field profiles for MV-size cable specimens. Calculated patterns and experimental data. V=+80 kV; T_a=68°C, T_b=46°C.

2) Polarity reversal

Accumulated charges can be released by the insulation when the external field is removed and the insulation short-circuited. However, this process can last quite a long time, depending on the type of insulation and on the temperature. In general, charge depletion is much longer for polymeric insulation than for oil-paper insulation.

A consequence of this phenomenon is that the accumulated charges will be kept within the insulation also when the external DC voltage is removed or when the value of the external DC voltage changes. The inversion of the voltage polarity in HVDC cables is a practical example of such a situation. In this particular case, the insulation experiences the sum of the space charge field and the field induced by the DC voltage, which direction has been inverted. This generally leads to a maximum field near the inner conductor of the cable. In the worst case, the maximum field can be as high as twice the maximum value of the Laplacian field.

In Figure 13, space charge profiles detected during a polarity reversal test are represented. The test has been performed according to the following procedure. Firstly, a voltage of +90 kV is applied for $20 \cdot 10^4$ s (5.6 hours). Then, the voltage is removed and the cable conductor grounded. At this point, a few measurements of space charge are done with the cable conductor at earth potential. After removing the earth connection, a voltage of –90 kV is applied. The operations necessary for inverting the voltage polarity and performing the measurements with conductor at earth potential take about two minutes.
Figure 14 shows the electric field distributions corresponding to the space charge profiles in Figure 13.

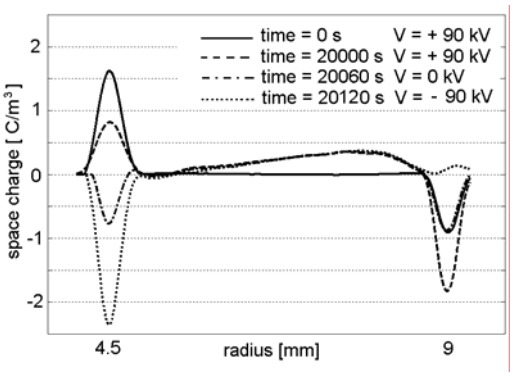

Figure 13: space charge profiles measured on a MV XLPE cable during a polarity reversal test. ΔT =20 °C.

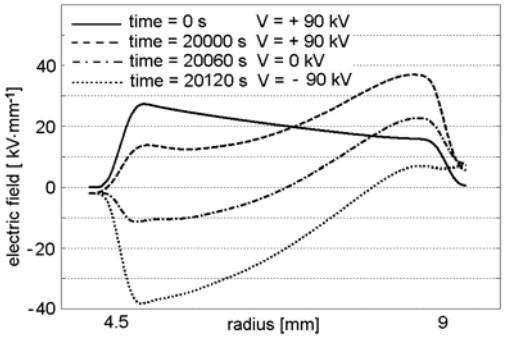

Figure 14: electric field distributions in a MV XLPE cable during a polarity reversal test. ΔT = 20 °C.

It is interesting to see that the highest electric stress cable experiences during the test is present at the inner conductor immediately after the reversal of the voltage polarity. The reason for this behavior is that immediately after the inversion of the voltage polarity, the distribution of space charge is almost unchanged. In fact, the time required for the change of the voltage polarity (120 s) is much shorter than the time the accumulated space charge needs to decay (tens of minutes – hours). So, also the space charge field associated to the internal charges remains practically the same. As a consequence, the superposition of the unchanged space-charge field and the applied field with direction reversed, results in a maximum field inside the cable of about 60% higher than the Laplace field, as shown in Figure 14.

CONCLUSIONS

A physical model, which is based on the macroscopic properties of the insulation, can qualitatively reproduce the space charge phenomena occurring in DC cables and interfaces.

Practical situations such as the presence of a temperature gradient across the cable system can be studied by means of the presented model.
Experimental results validated the fact that the conductivity of the insulation and its dependency on field and temperature have an important role in the charging behavior both at dielectric interfaces and within the insulation bulk.

Space charge measurements have been performed on MV-size XLPE cable specimens during a polarity reversal test. Measurement results point out that the accumulated charge is responsible for the field enhancement near the inner conductor after the inversion of the voltage polarity.

REFERENCES

[1] T. Maeno, H. Kushibe, T. Takada, C. M. Cooke, *"Pulsed electro-acoustic Method for the measurement of volume charge in e-beam irradiated PMMA"*, Proc. IEEE Conf. Electr. Insul. Diel. Phenom., pp. 389-397, 1985.
[2] L. A. Dissado, J. C. Fothergill, *Electrical degradation and breakdown in polymers*, published by Peter Peregrinus Ltd, ISBN 0-86341-196-7, 1992.
[3] R. Bodega, G.C. Montanari, P.H.F. Morshuis, *"Conduction current measurements on XLPE and EPR insulation"*, Proc. IEEE Conf. Electr. Insul. Diel. Phen., pp. 101-105, 2004.
[4] R. Bodega, *Space charge accumulation in polymeric high voltage DC cables*, PhD thesis Delft University of Technology, ISBN 90-8559-228-3, 2006.
[5] R. Coelho, *"Charges in non homogeneous dielectrics"*, Proc. IEEE Conf. Electr. Insul. Diel. Phen., pp. 1-10, 1997.
[6] D. Fabiani, G. C. Montanari, R. Bodega, P. H. F. Morshuis, C. laurant, L. A. Dissado, *"The effect of temperature gradient on space charge and electric field distribution of HVDC cable models"*, Proc. Int. Conf. Prop. App. Diel. Mat., 2006.
[7] M. Jeroense, P. H. F. Morshuis, *"Electric fields in HVDC paper-insulated cables"*, IEEE Trans. Dielectr. Electr. Insul., Vol. 5 No. 2, pp. 225-236, 1998.